NASA

Technical Memorandum 80320

Interpreting Vegetation Reflectance Measurements as a Function of Solar Zenith Angle

D. S. Kimes, J. A. Smith and K. J. Ranson

JULY 1979

National Aeronautics and
Space Administration

Goddard Space Flight Center
Greenbelt, Maryland 20771

INTERPRETING VEGETATION REFLECTANCE MEASUREMENTS AS A FUNCTION OF SOLAR ZENITH ANGLE*

D. S. Kimes
Earth Resources Branch
NASA Goddard Space Flight Center
Greenbelt, Maryland 20771 USA

J. A. Smith
K. J. Ranson
College of Forestry and Natural Resources
Colorado State University
Fort Collins, Colorado 80523 USA

July 1979

*This is a preprint of an article submitted to Photogrammetric Engineering and Remote Sensing.

GODDARD SPACE FLIGHT CENTER
Greenbelt, Maryland

INTERPRETING VEGETATION REFLECTANCE MEASUREMENTS AS A FUNCTION OF SOLAR ZENITH ANGLE*

D. S. Kimes
Earth Resources Branch
NASA Goddard Space Flight Center
Greenbelt, Maryland 20771 USA

J. A. Smith
K. J. Ranson
College of Forestry and Natural Resources
Colorado State University
Fort Collins, Colorado 80523 USA

ABSTRACT

An understanding of the behavior of vegetation canopy reflectance as a function of solar zenith angle is important to several remote sensing applications. Spectral hemispherical-conical reflectances of a nadir looking sensor were taken throughout the day of a lodgepole pine and two grass canopies. Mathematical simulations of both spectral hemispherical-conical and bi-hemispherical reflectances were performed for two theoretical canopies of contrasting geometric structure. These results and comparisons with literature studies showed a great amount of variability of vegetation canopy reflectances as a function of solar zenith angle. Explanations for this variability are discussed and recommendations for further measurements are proposed.

*This is a preprint of an article submitted to Photogrammetric Engineering and Remote Sensing.

CONTENTS

TABLES

ILLUSTRATIONS

ILLUSTRATIONS (Continued)

INTERPRETING VEGETATION REFLECTANCE MEASUREMENTS AS A FUNCTION OF SOLAR ZENITH ANGLE*

INTRODUCTION

An understanding of solar radiation interaction with vegetation canopies is necessary for accurately interpretating remotely sensed data. Broad and narrow-band spectral reflectance measurements of vegetation canopies are often used to characterize this solar interaction. Measured reflectance however, is a complex function of canopy constituent optical properties (Gates, 1970; and Knipling, 1970), canopy geometry (Kimes, et al., 1979b; and Ross, 1976), optical properties of the ground, atmospheric conditions (Kriebel, 1976; and Ross, 1976), solar zenith angle (Smith, et al., 1974; Kriebel, 1975; and Jarvis, et al., 1976), and sensor inclination and azimuthal view angles (Smith and Oliver, 1974; Kriebel, 1978; and Smith, et al., 1979).

Understanding canopy reflectance as a function of solar zenith angle is important for several remote sensing applications. For example, such knowledge can improve multitemporal vegetation classification by using sun-angle signature extension techniques (Smith, et al., 1975). At higher latitudes low sun-angles predominate and an understanding of the reflectance changes at low sun-angles would be beneficial. Diurnal reflectance trends are also important in photosynthetic and productivity studies.

To better understand these relationships, spectral reflectance measurements were obtained for several solar zenith angles for a lodgepole pine and two grass canopies. Mathematical simulations of the diurnal reflectance from theoretical vegetation canopies were performed. The instruments and methods used to obtain these data are described and the resulting trends presented and discussed. The results were also compared to other field measurements of vegetation canopies, and sources of variation are discussed.

*This is a preprint of an article submitted to Photogrammetric Engineering and Remote Sensing.

REFLECTANCE NOMENCLATURE

The two reflectance measurements which are most commonly reported in the literature for natural vegetation canopies are bi-hemispherical and hemispherical-conical reflectance. In this study a nadir looking sensor was used to measure the hemispherical-conical reflectance of vegetation canopies. The definitions of these reflectances are presented as follows. For clarity the standard nomenclature and symbolism for the basic radiometric quantities (e.g., radiance, irradiance, and exitance) as presented by Suits (1975) were used exclusively.

Bi-hemispherical reflectance (ρ^{H}) is defined as the ratio of the reflected exitance to the irradiance at the target surface. The hemispherical-conical reflectance (ρ^{C}) for a nadir looking sensor having a field of view of less than 2π steradians is measured as the ratio of the reflected exitance of a surface in the direction of the sensor's field of view (FOV) to the reflected exitance of a perfect reflecting horizontal lambertian surface in the direction of the sensor's FOV. The mathematical representation of the above measurements is given by:

$$\rho^{H} = \frac{\int_0^{2\pi}\int_0^{\frac{\pi}{2}} L_r(\theta_r, \phi_r)\cos\theta_r \, dw_r}{\int_0^{2\pi}\int_0^{\frac{\pi}{2}} L_i(\theta_i, \phi_i)\cos\theta_i \, dw_i} = \frac{M}{E} \qquad (1)$$

where θ_r, ϕ_r = The zenith and azimuth angles of the reflected sources respectively

θ_i, ϕ_i = The zenith and azimuth angles of the incident sources, respectively

L_r, L_i = The radiance values of the reflected and incident sources respectively as a function of θ and ϕ

dw_i = $SIN\theta_i \, d\theta_i \, d\phi_i$

dw_r = $SIN\theta_r \, d\theta_r \, d\phi_r$

M = reflected exitance

E = irradiance

and

$$\rho^C = \frac{\int_{\phi_1}^{\phi_2} \int_{\theta_1}^{\theta_2} L_r(\theta_r, \phi_r) \cos\theta_r \, dw_r}{\int_{\phi_1}^{\phi_2} \int_{\theta_1}^{\theta_2} \frac{A}{\pi} \cos\theta_i \, dw_i} \tag{2}$$

where A = The denominator of Equation (1).

$\phi_1, \phi_2, \theta_1, \theta_2$ = The azimuth and zenith angle limits of the sensor's steradian view.

Note that the denominator and numerator of Equations (1) and (2) represent what the sensor would measure from a reference panel (e.g., barium sulfate) and vegetation canopy respectively.

The bi-hemispherical (ρ^H) and hemispherical-conical (ρ^C) measurements are related to the bi-directional reflectance function (ρ^B) as described by Nicodemus (1970) and Kriebel (1976). The ρ^B function is

$$\rho^B(\theta_i, \phi_i; \theta_r, \phi_r) = \frac{d\, L_r(\theta_r, \phi_r)}{L_i(\theta_i, \phi_i) \cos\theta_i \, dw_i} \tag{3}$$

As stated by Kriebel (1976) the function is defined as the relation of that part of the total spectral radiance $dL_r(\theta_r, \phi_r)$ reflected into the direction θ_r, ϕ_r which originates from the direction of incidence θ_i, ϕ_i, to the total spectral irradiance $L_i(\theta_i, \phi_i) \cos\theta_i \, dw_i$ impinging on a surface from the direction θ_i, ϕ_i. This particular bi-directional reflectance function (ρ^B) is a unique characterization of a surface and is not dependent on the irradiance distribution as are a number of other bi-directional functions presented in the literature.

From Equation (3) it follows that

$$L_r(\theta_r, \phi_r) = \int_0^{2\pi} \int_0^{\frac{\pi}{2}} \rho^B(\theta_i, \phi_i; \theta_r, \phi_r) \, L_i(\theta_i, \phi_i) \cos\theta_i \, dw_i \tag{4}$$

As a consequence, ρ^C and ρ^H are dependent on both the bi-directional reflectance function ρ^B and the solar irradiance distribution (Equations (1) and (2)). From these equations it is important

to note that hemispherical-conical reflectance (ρ^C) which is most commonly utilized in remote sensing research is not a physical parameter uniquely determined by a particular vegetation canopy but is dependent on the anistropic distribution of sky irradiance. It is the bi-directional reflectance function together with information on the anistropic distribution of sky irradiance which ultimately determines how vegetation canopy ρ^C and ρ^H reflectances will behave under various solar irradiance conditions. Bi-directional reflectance is a function of a number of geometric and optical characteristics of the canopy components as discussed by Oliver and Smith (1974) and Ross (1976). Kriebel (1974, 1978) presents spectral bi-directional reflectance values for four vegetation canopies.

A description of the above and other types of reflectance measurements are presented by Judd (1967) and Nicodemus (1970). The reflectance measurements can be distinquished as broad band (ρ^H, ρ^C, ρ^B) or spectral ($\rho^H_\lambda, \rho^C_\lambda, \rho^B_\lambda$) reflectance. The variability within and between these reflectance measurements are explored below. In addition, throughout this paper ρ^C_λ will refer to a nadir sensor angle.

INSTRUMENTATION AND METHODS

Both field and simulated data were obtained. In all field experiments a scene recording radiometer (SRR) as described by Berry, et al., (1978) was used to obtain spectral hemispherical-conical measurements (ρ^C_λ) of vegetation canopies. The SRR was suspended on support cables attached to two 15m towers which allowed nadir looking measurements with a field of view of 22.5° from above the canopy to be obtained. The optics consisted of a six narrow band interference filter wheel interfaced to a Hasselblad EL500 camera which provided a photographic record of the scene. All filtered spectral data were referenced to a horizontal barium sulfate panel to provide reflectance values. Filters used were centered at 4800, 5500, 6750, 7300, 8000, and 9600 Å and had a half width bandpass of 100 Å.

Four experiments were performed at two field sites to evaluate the spectral hemispherical-conical reflectance (ρ_λ^C) of various targets with changing solar zenith angle. The targets and date of measurements at site 1 were: lodgepole pine with a grass understory (August 4, 1976) and open meadow (August 6, 1976). At site 2 a grass community was measured (April 20, 1978 and May 18, 1978). In all experiments the sensor was nadir looking and a constant sensor position on the tower system was maintained. Target radiance and barium sulfate panel radiance data were taken frequently throughout the day and the corresponding measurements were ratioed to obtain the ρ_λ^C values.

A description of the two study sites was as follows: Site 1 was located southeast of Leadville, Colorado, in the northeastern section of the Iron Hill area at an elevation of approximately 3,322 m. The 45.7 m long transect defined by the tower system was oriented at 60° and maintained a constant slope and aspect of 5% at 045°. The vegetation gradated from a relatively dense lodgepole pine stand to an open, grass-covered clearing. Average height of the lodgepole pine stand was approximately 6.1 m. Canopy density was variable, ranging from 80% crown closure to the open meadow previously mentioned. The meadow was populated with rush (Juncus sp.) and sedge (Carex sp.). A more detailed description of the site was presented by Heimes and Smith (1977). A description of the geometric structure of the lodgepole pine canopy was presented by Kimes, et al., (1979a).

Site 2 was located west of Fort Collins, Colorado, at an elevation of 1,570 m at the Colorado State Forest Service Nursery. The towers at each end of the transect were 9 m high. Vegetation along the transect consisted of grasses which included fescue (Festuca), bluegrass (Poa), sedge (Carex), wheatgrass (Agropyron) and brome (Bromus). A more detailed description of the site was presented by Ranson, et al., (1978).

A solar radiation vegetation canopy (SRVC) model was utilized to simulate the ρ_λ^C and ρ_λ^H reflectances for various theoretical vegetation canopies. The SRVC model is a Monte Carlo model

which physically accounts for variations in direct/diffuse solar irradiance ratios, solar zenith angle, leaf angle geometry, leaf area indices (LAI), leaf spatial dispersion, and leaf and soil optical properties (Oliver and Smith, 1974). Several vegetation canopies were simulated with various geometric structures and LAI for a photosynthetically active spectral wavelength (0.68μm). The entire procedure and canopy absorption results are presented by Kimes, et al., (1979c). Two canopy geometries were simulated: an erectophile (mostly erect leaves) and planophile (mostly prostrate leaves) as described by DeWit (1965). These canopies were simulated for LAI of 1.0, 4.0, and 7.0. The simulated results were compared with field measurements and are presented in this study.

Finally, literature studies on vegetation reflectance trends as a function of solar zenith angles were compared with the results of the above experiments.

RESULTS AND DISCUSSION

Figures 1a and b present the 0.68 and 0.80μm band hemispherical-conical reflectances (ρ_λ^C) as a function of solar zenith angle for the lodgepole pine and meadow at site 1. These data were acquired on August 4, 1976, from 0657 to 1400 hours mountain daylight time (MDT) and August 6, 1976, from 0815 to 1558 hours MDT, respectively. The arrows denote the sequence of data points from morning to afternoon. For both canopies ρ_λ^C increased with decreasing solar zenith angle except for the 0.80μm band of the meadow in the morning. The meadow ρ_λ^C values were lower in the afternoon with respect to the morning and the opposite trend was apparent for lodgepole pine. All of the above ρ_λ^C measurements at site 1 were taken when the direct solar path was free of clouds. Consistently, there was a build up of cumulus clouds around noon which continued into the afternoon. The experiments were terminated when cloud cover did not permit a direct solar path free of clouds.

Figure 2a and b presents the measured ρ_λ^C results as a function of solar zenith angle for the grass community at site 2 on April 20, 1978, and May 18, 1978. The April and May data were collected from 0856-1715 MDT and 1015-1947 MDT, respectively. Data for both the 0.68μm

and 0.80μm bands are presented. Both of these experiments were executed under rapidly changing sky conditions. Cumulus clouds partially or totally obscured the sun at various times throughout the measurement periods. Accordingly, there was a relatively large amount of variability in the data. No dominating ρ_λ^C trends occurred as a function of solar zenith angle with exception of the 0.68μm band on May 18, which showed a slight increase in reflectance with decreasing solar zenith angle.

The SRVC simulated ρ_λ^C reflectance for a nadir looking sensor and the ρ_λ^H reflectance for an erectophile and planophile canopy of three LAI values are shown in Figure 3a, b, c, and d. These results showed that for LAI of 1.0 and 4.0 of the erectophile canopy the ρ_λ^C decreased with increasing solar zenith angle (Figure 3a). However, the ρ_λ^H for all three LAI values tended to increase with increasing solar zenith angle (Figure 3b). These differences arose from anistropic scattering by the vegetation canopy into off-nadir view angles. The effect can be correctly quantified by the bi-directional reflectance function as presented by Kriebel (1976, 1978) and discussed below. In contrast, the ρ_λ^C for the erectophile canopy of an 7.0 LAI increased with increasing solar zenith angle (Figure 3a). Subtle geometric and optical effects of the soil and canopy accounted for this discrepancy as will be discussed later.

Grass canopies such as measured in this study tend to assume erectophile geometries (Oliver and Smith, 1974). The measured results of the meadow (Figure 1b) showed ρ_λ^C both increasing and decreasing with increasing solar zenith angle.

The geometry of lodgepole pine was intermediate between a planophile and erectophile canopy as measured by Kimes, et al., (1979a). Kimes, et al., (1979b) have used the SRVC model to simulate ρ_λ^C as a function of solar zenith angle for the specific geometric and optical properties of the lodgepole pine canopy at site 1. Simulated ρ_λ^C decreased slightly as solar zenith angle increased as was shown by the measured data (Figure 1a).

The simulated results of the planophile canopies were much less variable than the erectophile canopy (Figure 3c, d).

The diurnal reflectance results from this study were compared to previous studies. These comparisons showed a great deal of variability in diurnal reflectance trends. This variability and explanations for it will be presented under the headings of ρ^C, ρ^H, and ρ^B reflectance.

ρ^C Reflectance

In general the measured and simulated ρ_λ^C results for the vegetation canopies supported a trend of decreasing ρ_λ^C with increasing solar zenith angle. There were exceptions, however, as noted above.

Smith, et al., (1975) have measured ρ_λ^C of wheat using an Exotech ERTS Radiometer. The spectral reflectance of three plots were sampled using the four Landsat MSS bands. Mean ρ_λ^C values for various solar zenith angles were recorded for three different wheat stages: tillering (March 20), jointing (April 23), and heading (May 20). Figure 4a, b, and c showed the mean ρ_λ^C values of each wheat stage for bands 5 and 7 (0.6-0.7μm and 0.8-1.1μm, respectively) as a function of solar zenith angle. In addition, the mean LAI of each stage was presented. Although the data in Figure 4a, b, and c were collected for only a few solar zenith angles, the results showed temporal variation of the diurnal trajectories of wheat. The measured geometric structure of the three stages of wheat approximated erectophile geometries (Smith, et al., 1975). The diurnal trajectories both increase and decrease with increasing solar zenith angle. Explanations for this variability are as follows.

Kriebel (1978) has shown that the bi-directional reflectance functions for vegetation canopies were generally non-isotropic in nature. As a consequence, ρ_λ^C variations arise from a changing anistropic irradiance field since the observed ρ_λ^C is an integration of the bi-directional reflectance values (ρ_λ^B) for the near nadir reflectance angles and all incident radiation angles (Equations 2 and 4). Each of these ρ_λ^B values must be weighted by the distribution of the incoming solar

irradiance field. This weighting phenomena may account for the wide variability in measured ρ_λ^C seen on partly cloudy days (Fig. 2a, b). It is precisely this effect that is responsible for the changing ρ_λ^C as a function of solar zenith angle on clear days. Specifically, the data from Kriebel (1978) indicate non-lambertian behavior for the four vegetated surfaces: savanah, bog, pasture land, and coniferous forest. Assuming that the sun is the primary radiant source on a clear day, the ρ_λ^C can be approximated by $\rho_\lambda^B(\theta_s, \phi_s; \theta_o, \phi_o)$ where θ_s, ϕ_s denote the solar zenith and azimuth angles respectively and θ_o and ϕ_o denote the viewing angle of a nadir sensor (Equation 3). The $\rho_\lambda^B(\theta_s, \phi_s; \theta_o, \phi_o)$ values for the four vegetation types did not follow any consistent trend with increasing solar zenith angle. Thus from the results of this study and the cited literature one may expect ρ_λ^C trajectories of vegetation as a function of solar zenith angle to be relatively variable due to the different bi-directional functions of plant canopies and variation in atmospheric conditions throughout the day.

There was a significant deviation between morning and afternoon reflectances. In some instances the morning ρ_λ^C were higher than those in the afternoon (meadow, Figure 1b) and in other instances the opposite is true (lodgepole, Figure 1a). Such an effect was not explored using the SVRC model because azimuthal symmetry is mathematically assumed. Ripley and Redmann (1976) found for a grassland canopy that the reflectance was considerably higher during the afternoons than in the morning for the same solar zenith angle. They propose that a portion of the observed variation is caused by canopy geometry in which preferential azimuthal orientation of the leaves was assumed due to a preferential wind direction. The authors also suggested that plant water content, leaf rolling, and atmospheric conditions may also be involved. If such variations in canopy geometry caused the above phenomena, the variations in canopy geometry due to temporal, spatial, stress, and wind variations may also account for the contrasting diurnal reflectance trajectories seen in this study and others.

Variations in reflectance trajectories can be explained by other subtle geometric effects. For example, the simulated SRVC ρ_λ^C results of an erectophile canopy showed that for LAI values of

1.0 and 4.0 ρ_λ^C decreased with increasing solar zenith angle (Figure 3a). However, the opposite trend was observed for an LAI of 7.0. The radiation transfer within vegetation canopies for highly absorptive wavelengths such as the simulated wavelength used in this study (0.68μm) is largely controlled by the probability of gap (PGAP) in the canopy as a function of source angle. Thus, the above variability can be explained as follows. At low LAI the PGAP to the ground varies greatly as a function of view angle. This variation for high LAI is small (Table 1). The spectral reflection (ρ_λ) and transmission (τ_λ) for the canopy components and ground were ρ_λ = 0.8, τ_λ = 0.4, and ρ_λ = 0.11, τ_λ = 0.00, respectively (Kimes, et al., 1979c). Thus, ground reflectance was significantly higher than the canopy components. The PGAP for a small zenith angle and a LAI of 1.0 was high. As a consequence, the observed ρ_λ^C for small solar zenith angles should be high due to the relatively high contribution of ground reflectance. At large solar zenith angles the PGAP to the ground was small and the observed ρ_λ^C is low due to the relatively small contribution of ground reflectance. For an LAI of 7.0 the PGAP was relatively constant with zenith angle and as a consequence the above effect was dominated by other geometric interactions.

ρ^H Reflectance

Although ρ^H reflectances were not measured directly in this study, a large amount of data has been collected for vegetation canopies by other researchers. These reflectance measurements are compared with the results of this study. It is important to understand the inherent differences between ρ^H and ρ^C measurements.

The simulated results within this study showed that the ρ_λ^C and ρ_λ^H for the erectophile canopy as a function of increasing solar zenith angle decreased and increased, respectively. These differences were explained by the anistrophic bi-directional reflectance function of the simulated vegetation canopy. Equations (1), (2), and (4) showed the ρ^H and ρ^C dependence on the bi-directional reflectance function. According to measurements from Coulson (1966) and Kriebel (1978) and simulated results from Oliver and Smith (1974), the nadir spectral reflectance was generally lower than all off nadir spectral reflectances for any given source direction. As a consequence, one

would expect the nadir ρ_λ^C to be lower than the corresponding ρ_λ^H reflectance. Such information is important for several applications. For example, accurate estimation of ρ^H for global surfaces is important in calculating the planetary heat budget. Eaton and Dirmhirn (1979) have developed coefficients to estimate bi-hemispherical measurements from hemispherical-conical measurements for several target types. The purpose of these coefficients were to improve the prediction of ρ^H from the conical radiance values from space platforms.

Coulson and Reynolds (1971) have measured ρ_λ^H as a function of solar zenith angle of six vegetation canopies for six discrete wavelengths in the visible and near infrared regions. The authors found that the reflectances of most surfaces reached a maximum at solar zenith angles of 80–70° and in general ρ_λ^H decreased with decreasing solar zenith angle. The authors suggested that these trends are a result of the effects of both canopy structure and the changing ratio of direct to diffuse light throughout the day. The magnitude of these independent effects on ρ_λ^H are not known.

There are a large number of studies which showed a decreasing broad band bi-hemispherical reflectance (ρ^H) with decreasing solar zenith angle for vegetation canopies (Rijks, 1967; Davies and Buttimor, 1969; Idso, et al., 1969; Proctor, et al., 1972; Ripley and Redmann, 1976; among others). These studies used sensors sensitive to the visible and/or near IR regions. A typical parabolic curve from Proctor, et al., (1972) is presented in Figure 5. As previously discussed, the changing ρ_λ^C as a function of solar zenith angle was largely due to the non-lambertian nature of the bi-directional reflectance function, the changing solar irradiance field, and the directional field of view of the sensor. However, the parabolic relationship seen in Figure 5 for ρ^H reflectance as a function of solar zenith angle cannot be explained by the above directional considerations since ρ^H is a hemispherical measurement integrating overall view angles. Other geometric effects must be operating.

One explanation which is often presented is that the probability of a gap through the vegetation components in the upper layers is generally lowest at the larger solar zenith angles. As a

consequence, less radiant flux will be attenuated and absorbed by the soil and lower layers of the canopy and a greater bi-hemispherical reflectance will occur at the larger solar zenith angles. This is a simplified explanation of some very complex radiation transfers within vegetation canopies particularly in the near infrared region where strong multiple scattering occurs.

Secondly, studies which measured broad band ρ^{H} may introduce several sources of error. For example, one source of error which is commonly not considered when measuring broad band reflectance values is the effects of variations in the spectral quality of solar irradiance as a function of solar zenith angle and atmospheric conditions. When this variation is systematic in nature as a function of solar zenith angle, false reflectance trends can occur. As presented in the Appendix, simulated results showed that for a particular theoretical vegetation canopy the calculated bi-hemispherical reflectance (ρ^{H}) may increase as much as 25% from small to large solar zenith angles due to variations in the spectral quality of the solar irradiance.

Instrumentation error can also introduce systematic errors which cause false reflectance curves as a function of solar zenith angle. For example, using an Eppley pyranometer on an alfalfa canopy, Brown, et al., (1970) showed particularly that at greater solar zenith angles extraneous light (outside the normal 2π steradians) reached the sensor. The absolute reflectance error between a shaded sensor which reduced this extraneous light and an unshaded sensor is shown in Figure 6. This error can clearly introduce erroneous ρ^{H} trends as a function of solar zenith angle.

ρ^{B} Reflectance

In this article a specific ρ^{B} function as presented by Kriebel (1976) has been emphasized because the function was independent on the anistropic irradiance field. However, there are a number of studies which have made other types of bi-directional measurements on a variety of material types, for example, Egbert and Ulaby (1972), Eaton and Dirmhirm (1979), and Rao, et al., (1979) among others.

The trends and magnitudes of these studies suggested that these functions are highly variable and dependent on target types, geometric structure of targets, and the solar irradiance field. These studies attempted to explain some of the variability in terms of the optical and geometric characteristics of the vegetation canopies. However, to date there has been a lack of general understanding of the nature of the physical radiant interactions which take place in vegetation canopies in terms of the bi-directional function ρ_λ^B which is independent of the solar irradiance field.

CONCLUSIONS AND RECOMMENDATIONS

The wide variability seen in diurnal reflectance trends are caused by variations in anistropic sky irradiance, canopy component geometry and optical properties, and type of reflectance measurement. In addition, systematic errors in instrumentation and spectral integration can cause false diurnal reflectance trends. In most cases there is a lack of information concerning the effect of these variables on the magnitude of observed reflectance.

Considering the large number of possible permutations of variables affecting diurnal reflectance trends, we believed that future studies should be designed to relate observed diurnal reflectance trends to the physical characteristics of the canopy and irradiance field. Collecting reflectance data only would be undesirable. Further decoupling the effects of the anistropic irradiance and the anistropic reflectance of the canopy on canopy reflectance measurements must be accomplished before a more complete understanding of diurnal reflectance trends can be obtained.

It is unlikely that the variations in diurnal reflectances of vegetation canopies will be clearly understood until bi-directional measurements as suggested by Kriebel (1978) are more commonly derived and related to the geometric structure and optical properties of the canopy constituents.

ACKNOWLEDGMENTS

This work was supported in part by the U.S. Army Research Office under Contract No. DAAG 29-78-G-0045 and by the U.S. Forest Service under Cooperative Agreement 16-741-CA.

REFERENCES

Berry, J. K., F. J. Heimes, and J. A. Smith, 1978. A portable instrument for simultaneous recording of scene composition and spectral reflectance. Optical Engineering 17 (2): 143–146.

Brown, K. W., N. J. Resenberg, and P. C. Doraiswamy, 1970. Shading inverted pyranometer and measurements of radiation reflected from an alfalfa crop. Water Resources Res. 6: 1782–1786.

Coulson, K. L., 1966. Effects of reflection properties of natural surfaces in aerial reconnaissance. Applied Optics, 5(6): 905–917.

Coulson, K. L. and D. W. Reynolds, 1971. The Spectral Reflectance of Natural Surfaces. J. of Applied Meteorology, 10: 1285–1295.

Davies, J. A. and P. H. Buttimor, 1969. Reflection Coefficients, Heating Coefficients and net radiation at Simcoe, Southern Ontario. Agric. Met. 6: 373–386.

deWit, C. T., 1965. Photosynthesis of leaf canopies. Agric. Res. Rept. 663. Wageningen, Netherlands, Chapter 4.

Eaton, F. D. and I. Dirmhirn, 1979. Reflected irradiance indicatrices of natural surfaces and their effect on Albedo. Applied Optics, 18:(7) 994–1008.

Egbert, D. D. and F. T. Ulaby, 1972. Effects of Angles on Reflectivity. Photogrammetric Engineering 1972: 556–564.

Gates, D. M., 1970. Physical and physiological properties of plants. In: Remote Sensing with Special Reference to Agriculture and Forestry. National Academy of Sciences, Washington, D.C.

Gates, D. M., H. J. Keegan, J. C. Schleter, and V. R. Weidner, 1965. Spectral properties of plants. Applied Optics, 4: 11–20.

Heimes, F. J. and J. A. Smith, 1977. Spectral variability in mountain terrain. Final Report. USDA Rocky Mountain Forest and Range Experiment Station. Cooperative Agreement 16-625-CA. 115 p.

Idso, S. B., J. L. Hatfield, R. J. Reginato, and R. D. Jackson, 1978. Wheat yield estimation by albedo measurement. Remote Sensing of Environment 7: 237-276.

Idso, S. B., D. G. Baker, and B. L. Blad, 1969. Relations of radiation fluxes over natural surfaces. Quart. J. R. Met. Soc. 95: 244-257.

Jarvis, P. G., G. B. James and H. H. Landsberg, 1976. Coniferous forest. In: Vegetation and the Atmosphere, Vol. 2 (J. L. Monteith, ed) Academic Press, NY. 439 p.

Judd, D. B., 1967. Terms, definitions, and symbols in reflectometry. J. Optical Society of America 57 (4): 445-452.

Kimes, D. S., J. A. Smith, and J. K. Berry, 1979a. Extension of the optical diffraction analysis technique for estimating forest canopy geometry. Accept. Pub. Australian J. Bot.

Kimes, D. S., J. A. Smith, and K. J. Ranson, 1979b. Terrain Feature Canopy Modeling. Final Report, US Army Research Office. Grant Number: DAAG 29-78-G-0045. 160 p.

Kimes, D. S., K. J. Ranson, and J. A. Smith, 1979c. A Monte Carlo calculation of the effects of canopy geometry on PhAR absorption. Accept. Pub. Photosynthetica.

Knipling, E. G., 1970. Physical and physiological basis for the reflectance of visible and near-infrared radiation from vegetation. Remote Sensing of Environment 1: 155-159.

Kondrat'yev, K.Ya., 1965. Actinometry. Translation of "AKTINOMETRIYA" Gidometeorological Cheskoye Izdatel'Styo, Leningrad, 1965. National Aeronautics and Space Administration, Washington, D.C. November 1965. NASA TT F-9712.

Kriebel, K. T., 1974. The Spectral reflectance of a vegetated surface – II. An eight-channel radiometer for measurements of the reflected radiation field. Atmos. Phys. 47: 119–128.

Kriebel, K. T., 1976. On the variability of the reflected radiation field due to differing distributions of the irradiation. Remote sensing of Environment 4: 257–264.

Kriebel, K. T., 1978. Measured spectral bi-directional reflection properties of four vegetated surfaces. Applied Optics, 17 (2): 253–259.

Nicodemus, F. E., 1970. Reflectance nomenclature and directional reflectance and emissivity. Applied Optics 9 (6): 1474–1475.

Oliver, R. E. and J. A. Smith. A stochastic canopy model of diurnal reflectance. Final Report. US Army Research Office, Durham, North Carolina, DAH CO-4-74-60001. 105 p.

Proctor, J. T. A., W. J. Kyle, and J. A. Davies, 1972. The radiation balance of an apple tree. Can. J. Bot. 50 (8): 1731–1740.

Ranson, J. K., J. A. Kirchner, and J. A. Smith, 1978. Scene radiation dynamics, Vol. II. Final Report, Environmental Laboratory, U.S. Army Engineer Waterways Experiment Station. DACW 39-77-C-0073. 74 p.

Rao, V. R., E. J. Brach, and A. R. Mack, 1979. Bidirectional Reflectance of Crops and the Soil Contribution. Remote Sensing of Environment 8: 115–125.

Rijks, D. A., 1967. Water Use by Irrigated Cotton in Sudan. I Reflection of short-wave radiation. J. Appl. Ecol. 4: 561–568.

Ripley, E. A. and R. E. Redmann, 1976. Grassland. In: Vegetation and Atmosphere Vol. 2 (J. L. Monteith, ed.) Academic Press, New York, 439 p.

Ross, J., 1976. Radiative transfer in plant communities. In: Vegetation and the atmosphere, Vol. I Principles (J. L. Monteith, ed.). Academic Press, London.

Smith, J. A., J. K. Berry, and F. Heimes, 1975. Signature extension for sun angle, Vol. 1. Final Report. Earth Observations Division, NASA Johnson Space Center, NAS9-14467. Colorado State University, Fort Collins, Colorado. 105 p.

Smith, J. A. and R. E. Oliver, 1974. Effects of changing canopy directional reflectance on feature selection. Applied Optics, 13 (7): 1599-1604.

Smith, J. A., Tse Lie Lin, and K. J. Ranson, 1979. The Lambertian Assumption and Landsat Data. Accept. pub. Photog. Eng. and Remote Sens.

Suits, G. H., 1975. The nature of electro-magnetic radiation. In: Manual of Remote Sensing (R. G. Reeves, ed.). Amer. Soc. of Photo. Falls Church, VA.

Table 1

Probability of gap (PGAP) Through a Theoretical Erectophile Canopy of Leaf Area Index (LAI) Equal to 1.0, 4.0, and 7.0

LAI	Inclination View Angle Interval								
	0–10	10–20	20–30	30–40	40–50	50–60	60–70	70–80	80–90
1.0	0.0	0.0	0.0	0.214	0.392	0.520	0.613	0.680	0.720
4.0	0.0	0.0	0.0	0.002	0.024	0.073	0.142	0.214	0.268
7.0	0.0	0.0	0.0	0.0	0.001	0.010	0.033	0.067	0.100

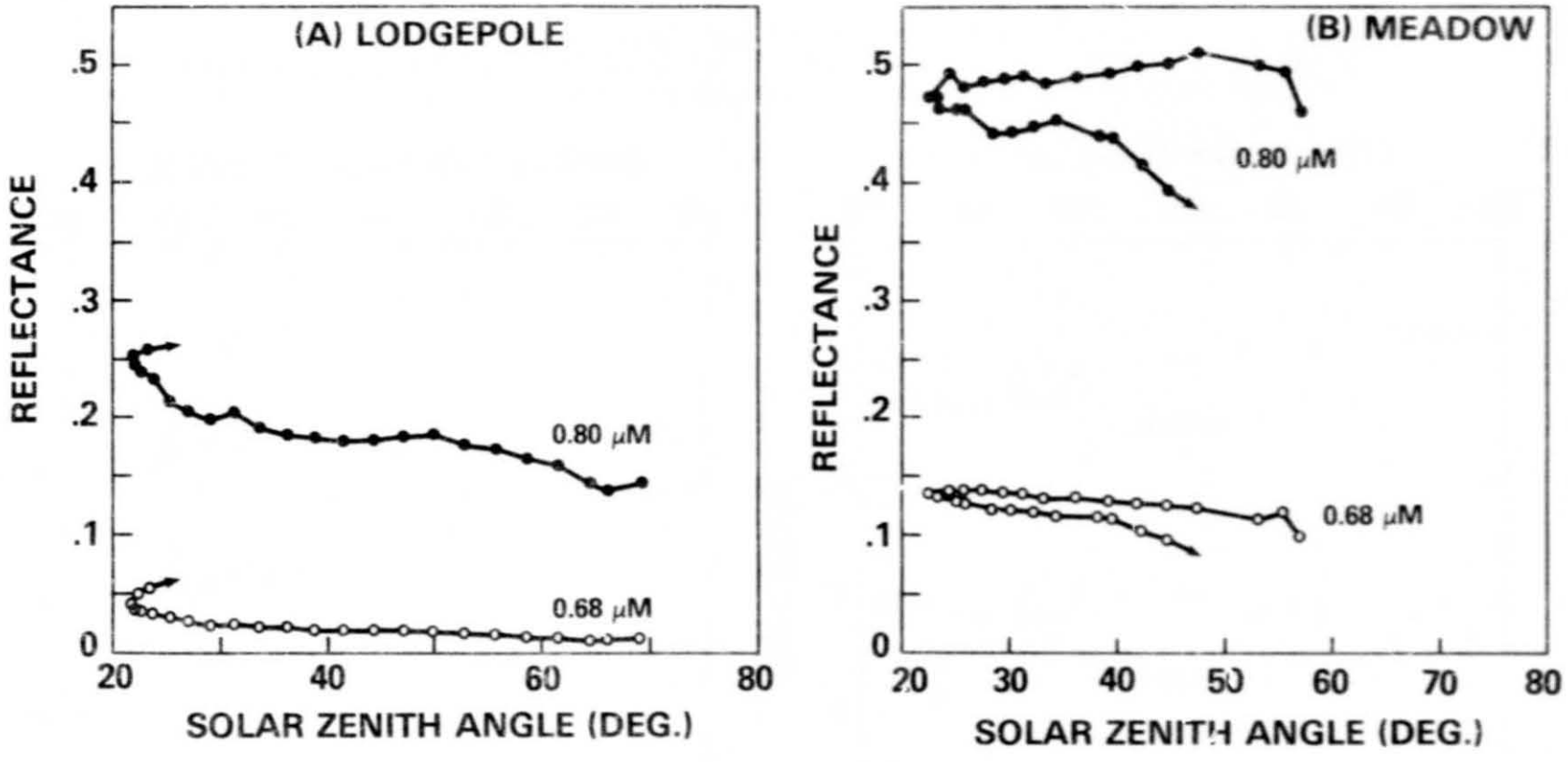

Figure 1. Spectral hemispherical-conical reflectance ρ_λ^C versus solar zenith angle of lodgepole pine (A) and meadow (B) at site 1 for the 0.68 and 0.80μm bands. Lodgepole and meadow data were collected 0657–1400 hours MDT August 4, 1976 and 0815–1558 hours MDT August 6, 1976.

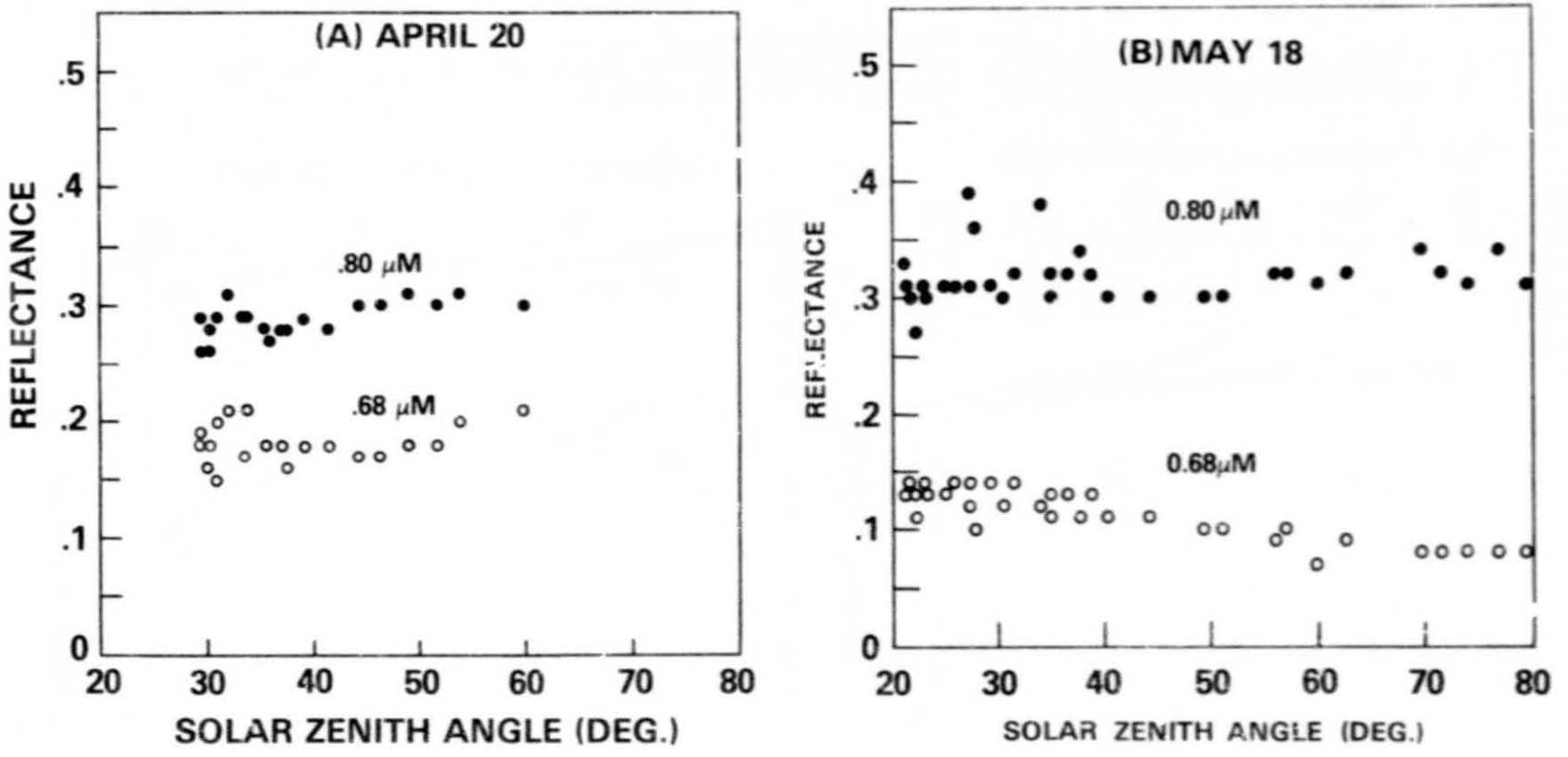

Figure 2. Spectral hemispherical-conical reflectance ρ_λ^C versus solar zenith angle of the grass canopy at site 2 for the 0.68 μm and 0.80 μm bands. Data were collected on April 20, 1978 (A) and May 18, 1978 (B) under variable cloud conditions.

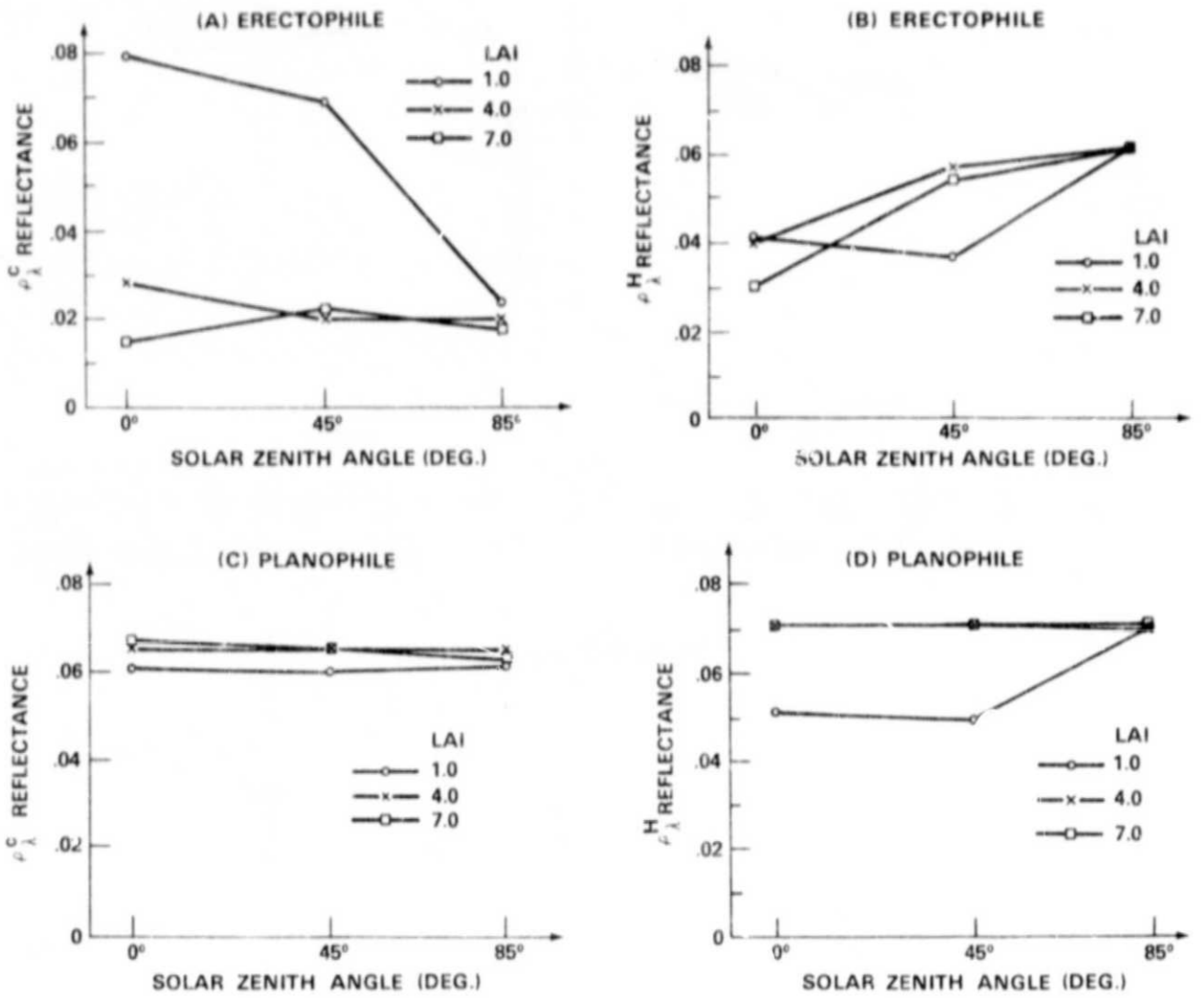

Figure 3. SRVC simulated spectral hemispherical-conical reflectance ρ_λ^C and bi-hemispherical reflectance ρ_λ^H as a function of solar zenith angle for theoretical erectophile and planophile canopies. A photosynthetically active wavelength (0.68 μm) was simulated for various leaf area indicies (LAI).

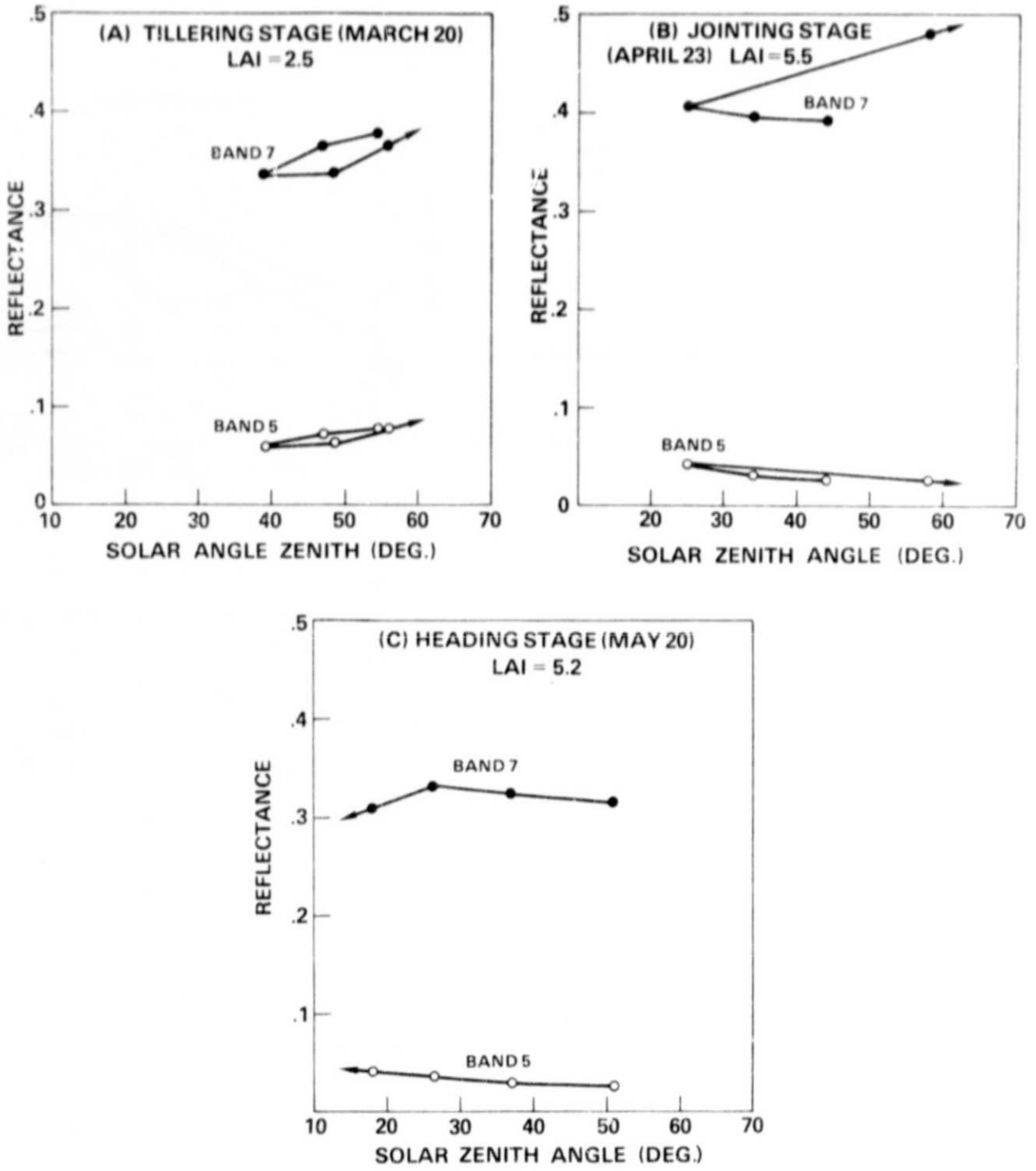

Figure 4. Mean spectral hemispherical-conical reflectance ρ_{λ}^{C} as a function of solar zenith angle for three wheat stages for Landsat bands 5 and 7.

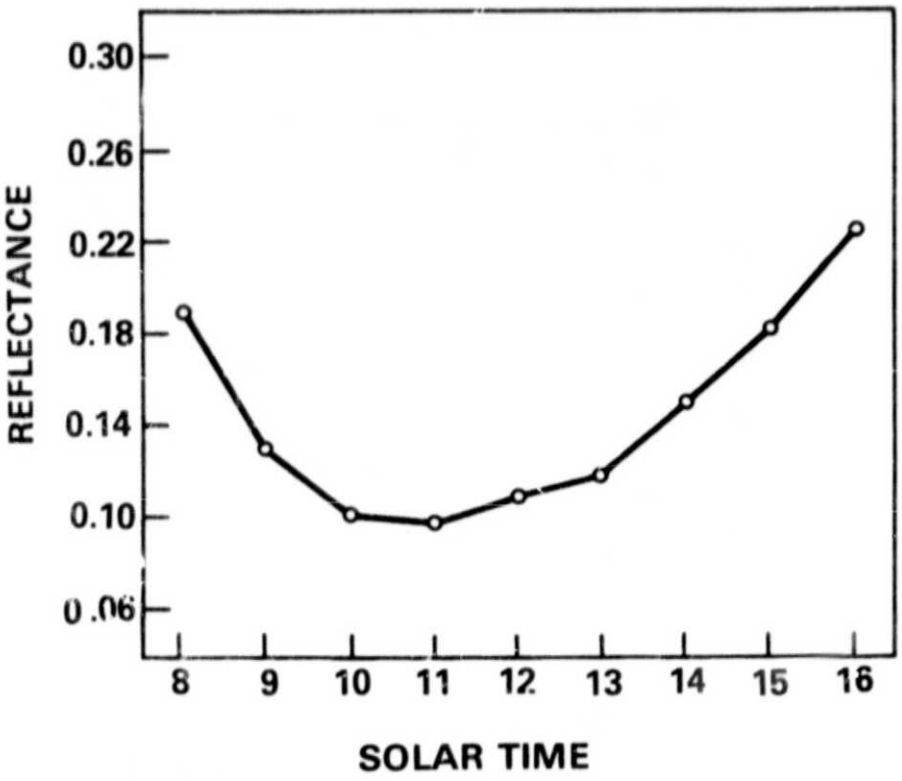

Figure 5. Diurnal bi-hemispherical reflectance ρ^H variations of an apple orchard. (After Proctor, et al., 1972).

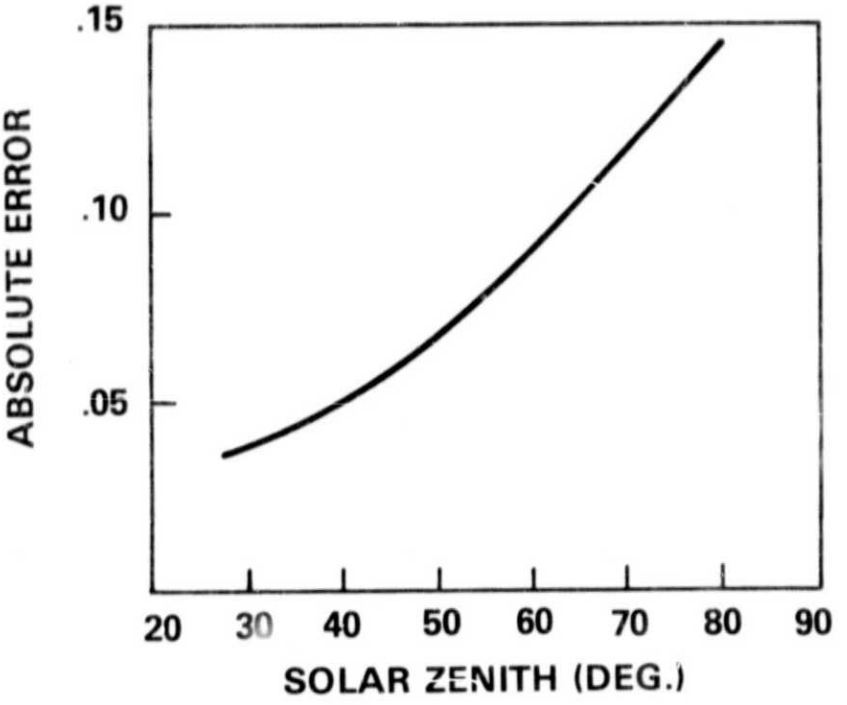

Figure 6. Absolute error of the unshaded minus shaded eppley pyranometer for measurements of shortwave bi-hemispherical reflectance ρ^H of an alfalfa canopy (derived from Brown, et al., 1970).

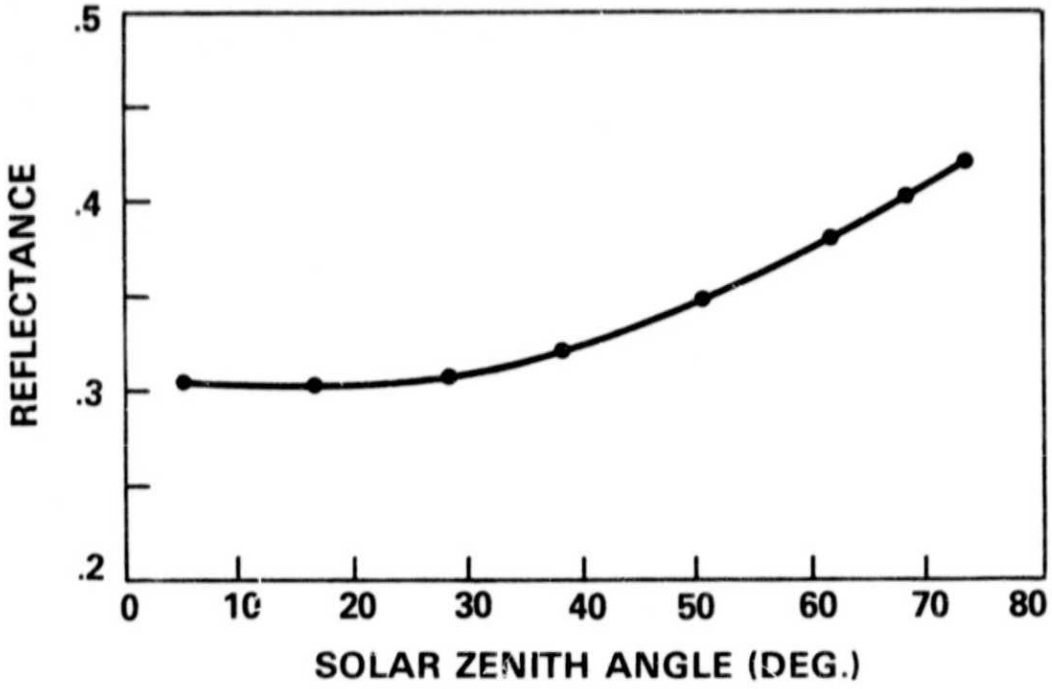

Figure 7. Simulated bi-hemispherical reflectance ρ^H from a theoretical vegetation canopy as a function of solar zenith angle.

APPENDIX

APPENDIX

When broad band bi-hemispherical reflectance (ρ^H) measurements are taken as a function of view angle, error is introduced due to the varying spectral quality of the solar irradiance. When this variation is systematic in nature as a function of solar zenith angle, false diurnal reflectance trends can occur. The following simulation was performed as an example.

First a basic distinction between broad band (e.g., entire solar spectrum) and discrete wavelength diurnal bi-hemispherical reflectance should be made. For very small discrete wavelength bands and ignoring path radiance and atmospheric transmission between the sensor and the target, the following ratio is measured:

$$\rho_\lambda^H = \frac{\rho_\lambda^H \cdot E_\lambda \cdot R_\lambda \cdot \Omega}{E_\lambda \cdot R_\lambda \cdot \Omega}$$

Where

ρ_λ^H = bi-hemispherical spectral reflectance of target

E_λ = hemispherical spectral irradiance

R_λ = spectral responsivity of detector

Ω = sensor related parameters

However, when using a broad band (e.g., total solar spectrum) such as used by Proctor, et al., 1972 and Idso, et al., 1978, one is measuring:

$$\rho^H = \frac{\int_{\lambda_1}^{\lambda_2} (\rho_\lambda^H \cdot E_\lambda \cdot R_\lambda \cdot \Omega)\, d\lambda}{\int_{\lambda_1}^{\lambda_2} (E_\lambda \cdot R_\lambda \cdot \Omega)\, d\lambda} \qquad (5)$$

Where;

λ_1, λ_2 = spectral limits of the effective detection of the sensor

ρ^H = measured broad band bi-hemispherical reflectance for the (λ_1, λ_2) interval.

For any given measurement period one wishes to measure a reflectance value for the entire spectral limits of the detector. However, it is clear that this measured value is dependent on the sensor's spectral responsivity R_λ and the solar irradiance E_λ. Indeed the E_λ is not a constant function but varies as a function of path length through the atmosphere and atmospheric conditions. Thus, it was hypothesized that diurnal reflectance trends as measured by broad solar band sensors may in some instances be only artifacts of the measurement procedure as reflected in Equation (5).

The above hypothesis was examined in the following manner. Initially it was assumed that an ideal detector was being used with $R_\lambda = 1.0$ units $\lambda\epsilon(\lambda_1, \lambda_2)$. In addition, for convenience the spectral solar irradiance was introduced as the product of the normalized spectral irradiance and the total irradiance. Thus, after the above transformations, Equation (5) becomes:

$$\rho^H = \frac{\int_{\lambda_1}^{\lambda_2} (\rho_\lambda^H \cdot E_\lambda^n \cdot E^t)\, d\lambda}{\int_{\lambda_1}^{\lambda_2} (E_\lambda^n \cdot E^t)\, d\lambda}$$

Where:

E^n = normalized solar irradiance function

$$\int_{\lambda_1}^{\lambda_2} E_\lambda^n\, d\lambda = 1.0$$

E^t = total solar irradiance in the (λ_1, λ_2) interval.

The above equation can be further reduced.

$$\rho^H = \int_{\lambda_1}^{\lambda_2} (\rho_\lambda^H \cdot E_\lambda^n)\, d\lambda \qquad (6)$$

Theoretical E^n functions were derived for several atmospheric path lengths as a function of solar zenith angle from data for a clear and dry atmosphere presented by Kondrat'yev (1965). The resulting curves are presented by Kimes, et al., (1979b). In addition, a typical reflectance curve of a leaf was utilized for ρ_λ^H as reported by Kimes, et al.; (1979b). This ρ_λ^H curve was held constant with changing solar zenith angle, thus isotropic reflectance of the canopy was assumed. Equation 6 was then numerically integrated over 34 discrete wavelengths. The results for several solar zenith angles are presented in Figure 7.

Note in Figure 7 that with a constant ρ_λ^H function we obtained an increase in total ρ^H due to a changing E^n function throughout the day. The shifts in the E^n function throughout a theoretical clear day weighted different portions of the ρ_λ^H function thus causing a changing total ρ^H. Different responsivity functions (R_λ) of the detector could in some cases increase this effect.

Such an artifact as discussed above can mask true reflectance changes of vegetational canopies. Gates, et al., (1965) have reported similar effects for individual leaf reflectance under clear and cloudy sky conditions. Although one may criticize the validity of the particular sky irradiance and plant reflectance curves utilized in this study, the above simulation does demonstrate that such effects can feasibly occur. The same effect can theoretically occur for broad band hemispherical-conical reflectance (ρ^C) measurements.

BIBLIOGRAPHIC DATA SHEET

1. Report No.	2. Government Accession No.	3. Recipient's Catalog No.
80320		

4. Title and Subtitle	5. Report Date
INTERPRETING VEGETATION REFLECTANCE MEASUREMENTS AS A FUNCTION OF SOLAR ZENITH ANGLE	6. Performing Organization Code: 923
7. Author(s): Kimes, D. S., J. A. Smith, K. J. Ranson	8. Performing Organization Report No.
9. Performing Organization Name and Address: Earth Resource Branch, Code 923, NASA/Goddard Space Flight Center, Greenbelt, Maryland 20771	10. Work Unit No.
	11. Contract or Grant No.
	13. Type of Report and Period Covered: TM
12. Sponsoring Agency Name and Address	14. Sponsoring Agency Code

15. Supplementary Notes

16. Abstract

An understanding of the behavior of vegetation canopy reflectance as a function of solar zenith angle is important to several remote sensing applications. Spectral hemispherical-conical reflectances of a nadir looking sensor were taken throughout the day of a lodgepole pine and two grass canopies. Mathematical simulations of both spectral hemispherical-conical and bi-hemispherical reflectances were performed for two theoretical canopies of contrasting geometric structure. These results and comparisons with literature studies showed a great amount of variability of vegetation canopy reflectances as a function of solar zenith angle. Explanations for this variability are discussed and recommendations for further measurements are proposed.

17. Key Words (Selected by Author(s))	18. Distribution Statement
Reflectance, Solar Zenith Angle, Vegetation	

19. Security Classif. (of this report)	20. Security Classif. (of this page)	21. No. of Pages	22. Price*
UN	UN		

*For sale by the National Technical Information Service, Springfield, Virginia 22161.